Receptance-based natural frequency assignment of a real fluid-conveying pipeline system with interval uncertainty

Lin Zhang[a], Tao Zhang[a,*], Huajiang Ouyang[b], Tianyun Li[a], Shike Zhang[b]

[a] School of Naval Architecture & Ocean Engineering, Huazhong University of Science and Technology

Wuhan, Hubei 430074, China

[b] School of Engineering, University of Liverpool

Liverpool L69 3GH, UK

E-mail: zhangt7666@hust.edu.cn

Abstract: The resonance problem of an industrial fluid-conveying pipeline system can be mitigated by shifting or assigning its natural frequencies. However, the desired natural frequencies are difficult to realize using typical numerical model-based parameter optimization technologies because of the modelling errors. Herein, the first theoretical and experimental study is reported on achieving desired natural frequencies of an industrial pipeline system by using measured receptances. This research involves the one-way fluid-structure interaction of the steady flow. On this basis, this paper considers the changeability of working conditions of the pipeline system and characterizes the uncertain flow speed as an interval uncertainty. The primary framework of the classic receptance method is employed, and a novel interval-based frequency assignment method is proposed. This method inherits the advantage of the receptance methodology, in which the determination of the optimal structural modifications entirely relies on the measured frequency response functions. More especially, the obtained stiffness modifications by using the proposed method can improve the robustness of the assignment results to uncertain flow speeds, and then actually achieved values of the assigned natural frequencies have a smaller perturbation. Several numerical examples demonstrate that the proposed method provides effective results. The application of the method to the modification of a real U-shaped fluid-conveying pipeline system gives experimental evidence of its effectiveness. The effective experimental results give the confidence to use the

receptance-based structural modification method to improve the dynamical behaviour of real structures.

Keywords: Fluid-conveying pipeline; natural frequency assignment; measured receptance; interval uncertainty.

1. Introduction

Fluid-conveying pipelines are widely used in aerospace, shipping, mechanical, nuclear power, civil engineering, and other fields. They convey fluid organically to ensure the normal operation of the whole system [1,2]. However, a fluid-conveying pipeline inevitably vibrates during service because of internal and external factors [3]. In particular, when the excitation frequency of the motor connected to the pipeline is close or equal to a natural frequency of the pipeline system, the vibration of the pipeline system is amplified, leading to malfunction or even failure of the pipeline and affecting the normal operation of the whole system [4]. Therefore, assigning the natural frequency of the pipeline to shift it away from the excitation frequency is a useful and frequently-used way to suppress pipeline vibration, on the premise that the excitation frequency of the equipment cannot be changed [5].

Generally speaking, the material and dimensions of a pipeline usually cannot be changed due to the requirements of pipeline design standards [6]. Therefore, parameter optimization of pipeline supports, especially their stiffness, has received extensive attention in recent years and is expected to remain a popular solution to the resonance problem of pipelines. As pioneers in the study of pipeline support parameters, Kwong and Edge [7] employed the transfer matrix method to calculate frequency response functions (FRFs) for a fluid-conveying pipeline system and used them as input data to optimize pipeline support locations and stiffness. Huang et al. [8] investigated the one-way fluid-structure interaction (FSI) (the effect of carried fluid on structure) in a straight pipeline by using the eliminated element-Galerkin method, calculated the natural frequency of the fluid-conveying pipeline with different support stiffness values, and derived its optimal stiffness for assigning the desired frequency from the calculation results. Ritto et al. [9] and Zhai et

al. [10] used the nonparametric probabilistic and refined response-surface methods, respectively, to analyse the effect of the carried fluid on the vibration characteristics of the fluid-conveying pipeline. Recently, Guo et al. [11] focused on the uncertainty of the pipe parameters, support parameters, and fluid parameters and proposed an uncertain frequency response surrogate function to evaluate the effect of those uncertainties on the frequency response. Moreover, Wu and Tijsseling [12], Herrmann et al. [13], Wang et al. [14], and Chai et al. [15] conducted some similar but valuable studies.

Regarding the abovementioned literature, it should be noted that natural frequency assignment or optimization of pipelines is mainly performed based on the probabilistic design method, which usually involves a numerical model [16,17]. However, industrial fluid-conveying pipeline systems are often equipped with multiple shock absorbers as elastic supports, and their carried fluid also interacts with the structure [18]. These complex factors make it difficult to establish an accurate numerical model of a fluid-conveying pipeline system [19]. Most researchers ignore or model simplistically the influence of these factors when establishing simulation models of pipeline systems [6,20], which allow optimization of pipeline support parameters in simulation but often perform poorly in practice. More importantly, the process of finding optimal solutions involves many data samples, so making natural frequency assignment is time-consuming even when using a simplified model of a fluid-conveying pipeline system.

In order to overcome the limitations of numerical models for optimization, the receptance method is employed in this study as the basis to solve the natural frequency assignment problem of fluid-conveying pipeline systems. The receptance method neither involves the numerical model of the structures under study nor requires complete physical information. Optimal modifications (such as stiffness modifications) can be directly acquired from experimental FRFs (receptance) at the modification-related locations. Based on the implementation, the receptance method can be further divided into structural modification by passive elements and active vibration control using sensors and actuators. Active control is not the focus of this study and thus will not be touched upon from this point onward. Interested readers may consult relevant studies [21-23].

Passive modification was comprehensively discussed by Mottershead and Ram in a review paper [24]. Focusing on rank-one modifications, they suggested several modification approaches, including mass modification, grounding spring modification, and connecting spring modification. Their systematic study serves as the foundation for applying and popularizing the receptance method. Çakar [25] extended the rank-one modifications to the case where some desired natural frequencies were kept unchanged after one or more mass and stiffness modifications. Ouyang et al. [26,27] introduced the convex optimization method in the receptance method to overcome the difficulty of solving higher-rank modifications. Their work ensures that the obtained modification can be physically realized by imposing constraints on the design variables, thereby enhancing the applicability of the receptance method. Recently, Liu et al. [28] summarized the general form of higher-rank structural modifications, thereby making them easier to implement and improving the practicability of the receptance method. Kyprianou et al. [29], Richiedei et al. [30], and Zhang et al. [31] further improved the receptance method and addressed its shortcomings.

Even though the receptance method has unique advantages in structural modification or optimization, early studies on the receptance method concentrated on theoretical verification due to the restriction of the backward testing techniques. With the progress of testing technology in recent years, many researchers have focused on solving practical engineering problems. Mottershead et al. [32] obtained the torsional FRFs of an aircraft tail via an attached X-shaped sub-structure and then calculated the required mass modification by using the receptance method. Zarraga et al. [33] shifted the natural frequency of a brake-clutch system by applying stiffness modification, thereby successfully suppressing friction noise. Tsai et al. [34] determined the required structural modifications of a geared rotor-bearing system to assign frequencies by only using the measured receptance.

Unlike the aforementioned studies, the structural modification of the industrial pipeline system is more complex since it involves the FSI. The FSI causes the dynamic behaviour of the fluid-conveying pipeline to change, and such changes are uncertain since an industrial pipeline usually has multiple working conditions (flow speeds) [9,35,36].

4

Consequently, the receptance matrix used in the calculation actually varies with flow speed and can be considered an uncertain matrix [11], and the objective of structural modification is no longer a deterministic function but an uncertain function, too. Therefore, this paper places emphasis on the variation of working conditions on the natural frequencies and utilizes the interval method [37,38] to describe the uncertainty of the FRFs caused by the uncertain flow speed. The objective function interval of the natural frequency assignment is converted to a linear combination of two deterministic objective functions based on the order relationship of the interval [39]. More importantly, multiple natural frequencies can be assigned by means of higher-rank modification, which makes the structural modification problem a multi-objective optimization problem (MOP). The non-dominated sorting genetic algorithm II (NSGA-II) [40] with good global convergence performance is adopted to find the optimal solutions for the MOP.

The focus of this study is on only utilizing the measured receptance to realize the assignment of multiple frequencies for real fluid-conveying pipeline systems. This paper is organized as follows: In Section 2, the theoretical model of the fluid-conveying pipeline involved in one-way FSI is derived, and the interval-based natural frequency assignment method is proposed by employing the basic framework of the classic receptance method. Section 3 introduces the experimental model of a U-shaped fluid-conveying pipeline system with elastic supports as well as its corresponding dynamic behaviour. In Section 4, the effectiveness of the receptance method on the pipeline system with a constant flow speed is demonstrated numerically and experimentally. Section 5 describes details of the structural modification of the pipeline system with an uncertain flow speed, in which the changeable flow speed is characterised as interval uncertainty and the proposed interval-based method is employed to achieve the robust assignment of its natural frequency. Finally, conclusions are presented in Section 6.

2. Natural frequency assignment method of the fluid-conveying pipeline system

2.1 Problem statement and basic assumptions

This work intends to overcome the limitations of numerical models and solve the following two problems.

Problem 1: Assign the desired natural frequencies of a real fluid-conveying pipeline system directly by using the measured FRFs (receptance).

Problem 2: Improve the robustness of the assigned natural frequencies to the uncertain flow speed (or changeable working conditions).

In order to deal with the abovementioned problems, the receptance method is employed as the basic theory, and the equation of motion for the fluid-conveying pipeline system is presented. Therefore, all important assumptions about the equation of motion are highlighted here:

(i) The pipeline system involved in this work is slender, that is, the outside diameter of the pipe is much smaller than the pipe length [41].

(ii) The carried fluid in the pipeline is incompressible, and the FSI is considered a one-way coupling. For a common steel fluid-conveying pipeline in the industry, the carried fluid influences the dynamic behaviour of the structure, while the effect of structure on carried fluid at low speeds is marginal and can be ignored [5,46].

(iii) The flow speed of the carried fluid in the pipeline changes according to different working conditions, while the flow is uniform and steady at any of the determined working conditions of the pipeline [11]. Moreover, it should be noted that flow variations caused by testing or other factors are regarded as uncertainty in the flow speed.

(iv) Only the linear vibration of the pipeline is concerned, and the nonlinear vibration is ignored [42].

(v) The effect of Coriolis force of fluid on the structure is considered, and the Poisson coupling and fluid friction are neglected [41].

6

2.2 Dynamic equation of the fluid-conveying pipeline system with one-way FSI

In the framework of the assumptions mentioned above, the plug flow model is used to describe the flow of the carried water [41]. The fluid-conveying pipeline system without any branches can be approximated as an assembly system consisting of *n* straight pipeline elements [2]. According to the extended Hamilton principle, the vibration of each fluid-conveying pipeline element is governed by following Eq. (1)

$$\int_{t_1}^{t_2} \delta(T_1 + T_2 - U)\mathrm{d}t = 0 , \tag{1}$$

where *t* represents time; T_1 and T_2 are the kinetic energy of the pipe wall and the carried fluid, respectively; *U* is the elastic potential energy of the pipe structure. The energies of all parts involved can be found in Ref [2].

By employing the wave method [43] or the transfer matrix method (TMM) [44-46] and the dynamic substructure assembly technology [41], the impedance matrix of the pipeline under free boundary conditions is obtained

$$\tilde{Z} \qquad \mathbf{M}_\mathrm{p} + \mathbf{M}_\mathrm{f})s^2 + (\mathbf{C}_\mathrm{p} + \mathbf{C}_\mathrm{f}(V))s + (\mathbf{K}_\mathrm{p} + \mathbf{K}_\mathrm{f}(V)) , \tag{2}$$

where *s* denotes the complex frequency; $\tilde{Z}$ represents the impedance matrix of the pipeline element, whose dimension is $6(n+1) \times 6(n+1)$ (since *n* straight pipeline elements have *n*+1 nodes in total, and each node has 6 degrees of freedom); $\mathbf{M}_\mathrm{p}$ and $\mathbf{M}_\mathrm{f}$ are the positive-definite mass matrices of structure and fluid, respectively; $\mathbf{K}_\mathrm{p}$ is the positive-definite bending stiffness matrix; $\mathbf{K}_\mathrm{f}(V)$ is the negative-definite fluid stiffness matrix; $\mathbf{C}_\mathrm{f}(V)$ is the fluid damping matrix (which is skew-symmetric), $\mathbf{C}_\mathrm{p} = \alpha\mathbf{M}_\mathrm{p} + \beta\mathbf{K}_\mathrm{p}$ is the Rayleigh damping matrix, in which α and β are the Rayleigh damping coefficients. Moreover, it should be noted that $\mathbf{K}_\mathrm{f}(V)$ and $\mathbf{C}_\mathrm{f}(V)$ are related to the flow speed *V* of the carried water and contain only zeros when $V = 0$ m/s.

Subsequently, the lumped masses and elastic supports (a kind of ground spring) connected to the pipeline are considered, and the equation of motion of the fluid-conveying pipeline system with a general boundary condition is established [44]

$$\mathbf{Z}(s,V)\mathbf{u}(s,V) = (\tilde{\mathbf{Z}} \qquad \mathbf{M}_b s^2 + \mathbf{K}_b))\mathbf{u}(s,V) = \mathbf{f}(s), \tag{3}$$

where $\mathbf{u}(s,V)$ and $\mathbf{f}(s)$ are the displacement and force vectors, respectively. $\mathbf{Z}(s,V)$ is the whole impedance matrix under a general boundary condition; $\mathbf{M}_b$ is the mass matrix of lumped masses attached to the pipeline nodes; $\mathbf{K}_b$ is the stiffness matrix of the elastic supports.

For an industrial fluid-conveying pipeline system ($V<10$ m/s), the fluid damping does not entail energy dissipation (this part of damping cannot lead to a real part of the complex frequency), and the complex frequency s can be approximate as jω [9]. Therefore, Eq. (3) can be rewritten as

$$\mathbf{Z}(\mathrm{j}\omega,V)\mathbf{u}(\mathrm{j}\omega,V) = (\tilde{\mathbf{Z}} \qquad \cdot(-\mathbf{M}_b\omega^2 + \mathbf{K}_b))\mathbf{u}(\mathrm{j}\omega,V) = \mathbf{f}(\mathrm{j}\omega), \tag{4}$$

where ω represents real frequency, and j is the imaginary unit. It should be stressed that the application $\mathbf{f}(s) \mapsto \qquad)$ (the symbol $\mapsto$ represents a mapping) is linear, but $V \mapsto \qquad)$ is nonlinear.

According to the orthogonality of vibration modes, the receptance matrix $\mathbf{H}(\mathrm{j}\omega,V)$ can be expressed as [47]

$$\mathbf{H}(\mathrm{j}\omega,V) = \mathbf{Z}^{-1}(\mathrm{j}\omega,V) = \sum_{i=1}^{N} \frac{\boldsymbol{\varphi}_i^L(V)\boldsymbol{\varphi}_i^R(V)}{-\omega^2 + 2\mathrm{j}\xi_i\omega_i(V)\omega + \omega_i^2(V)}, \tag{5}$$

where $\boldsymbol{\varphi}_i^L$ and $\boldsymbol{\varphi}_i^R$ are the ith left and right eigenvector, respectively; ω_i and ξ_i represent the ith natural frequency and the damping ratio, respectively. For arbitrary element $h_{pq}(\mathrm{j}\omega,V)$ in $\mathbf{H}(\mathrm{j}\omega,V)$, it is often called the displacement FRF and can be written as

$$h_{pq}(\mathrm{j}\omega,V) = \mathbf{e}_p\mathbf{H}(\mathrm{j}\omega,V)\mathbf{e}_q^{\mathrm{T}} = \sum_{i=1}^{N} \frac{\varphi_{pi}^L(V)\varphi_{qi}^R(V)}{-\omega^2 + 2\mathrm{j}\xi_i\omega_i(V)\omega + \omega_i^2(V)}, \tag{6}$$

where $\mathbf{e}_p$ is a $6(n+1)$-dimensional unit column vector where the pth element is one and the remaining ones are zeros. For arbitrary natural frequency ω_i, $h_{pq}(\mathrm{j}\omega_i,V)$ is theoretically the poles of the FRF $h_{pq}(\mathrm{j}\omega_i,V)$. Therefore, the natural frequencies in practice can be identified by picking the peaks of the obtained FRF.

The aforementioned Eqs. (4-6) theoretically demonstrate that the fluid-conveying pipeline system with a steady flow

(with a constant flow speed) can be approximated as a linear, lightly damped system, and the receptance method is theoretically suitable for its structure modification. Moreover, those equations can provide assistance in creating the theoretical model of a real pipeline and numerically proving the effectiveness of the proposed natural frequency assignment method.

2.3 Receptance-based natural frequency assignment method

According to Eq. (5), the free vibration equation of the fluid-conveying pipeline system can be expressed as

$$\mathbf{Z}(j\omega_i,V)\boldsymbol{\varphi}_i^R(j\omega_i,V) = (\tilde{} + (-\mathbf{M}_b\omega_i^2 + \mathbf{K}_b))\boldsymbol{\varphi}_i^R(j\omega_i,V) = \mathbf{0} \,. \tag{7}$$

Once again, ω_i is a real number and represents the ith natural circular frequency; $\boldsymbol{\varphi}_i^R(j\omega_i,V)$ is the corresponding ith complex right-eigenvector.

In this work, natural frequency assignment is realized by changing the stiffness of the elastic supports. Essentially, modifying their stiffness means adding an unsolved stiffness modification $\Delta\mathbf{K}$ to the original pipeline system. Hence, the free-vibration equation for the modified system becomes

$$(\mathbf{Z}(j\hat{\omega}_i,V)+\Delta\mathbf{K})\hat{\boldsymbol{\varphi}}_i^R(j\hat{\omega}_i,V) = \mathbf{0} \,, \tag{8}$$

where $\hat{\omega}_i$ is the ith natural frequency of the modified system, and $\hat{\boldsymbol{\varphi}}_i^R(j\hat{\omega}_i,V)$ is the corresponding ith complex right-eigenvector of the modified system.

Suppose that $\hat{\omega}_i$ is the desired natural frequency and already known from the industrial requirement. The target of the natural frequency assignment (*Problem* 1) is to find the required stiffness modifications to realize the desired frequency [24]. That is to say, the structural modification problem becomes an inverse problem of solving the required stiffness modification $\Delta\mathbf{K}$.

In order to solve the abovementioned inverse problem, both sides of Eq. (8) are pre-multiplied by the receptance matrix $\mathbf{H}(\hat{\omega}_i,V)=\mathbf{Z}^{-1}(j\hat{\omega}_i,V)$ of the original system at desired frequency $\hat{\omega}_i$ [24]. Eq. (8) can be rewritten as

$$(\mathbf{I}+\mathbf{H}(j\hat{\omega}_i,V)\Delta\mathbf{K})\hat{\boldsymbol{\varphi}}_i^R(j\hat{\omega}_i,V) = \mathbf{0}.$$ (9)

It should be stressed that stiffness modification $\Delta\mathbf{K}$ contains a large number of zero elements, and its rank (r) is equal to 5 in this study. Therefore, $\Delta\mathbf{K}$ can be expressed as [33]

$$\Delta\mathbf{K} = \sum_{x=x_1}^{x_r} \sum_{y=y_1(x_1)}^{y_r(x_r)} \Delta K_{xy}\mathbf{e}_x\mathbf{e}_y^{\mathrm{T}},$$ (10)

where ΔK_{xy} is a nonzero entry in the matrix $\Delta\mathbf{K}$, where x and y represent its row and column numbers, respectively. Meanwhile, set $\{x_1, \dots$ is identical to the set $\{y_1, \dots$ since $\Delta\mathbf{K}$ is a symmetric matrix.

Therefore, $\Delta\mathbf{K}$ can be rewritten with elementary transformations as follows

$$\Delta\mathbf{K} = \begin{bmatrix} 0 & 0 \\ 0 & \Delta\mathbf{K}_{rr} \end{bmatrix},$$ (11)

where $\Delta\mathbf{K}_{rr}$ is the unsolved stiffness modification matrix applied to the elastic supports; r is the number of elastic supports allowed to be modified.

Furthermore, Eq. (9) with the transformation of $\Delta\mathbf{K}$ can be rewritten as [28]

$$\left[\begin{bmatrix} \mathbf{I}_{(n-r)(n-r)} & \mathbf{0} \\ \mathbf{0} & \mathbf{I}_{rr} \end{bmatrix} + \begin{bmatrix} \mathbf{H}_{(n-r)(n-r)}(j\hat{\omega}_i,V) & \mathbf{H}_{(n-r)r}(j\hat{\omega}_i,V) \\ \mathbf{H}_{r(n-r)}(j\hat{\omega}_i,V) & \mathbf{H}_{rr}(j\hat{\omega}_i,V) \end{bmatrix} \begin{bmatrix} \mathbf{0} & \mathbf{0} \\ \mathbf{0} & \Delta\mathbf{K}_{rr} \end{bmatrix} \right] \begin{bmatrix} \hat{\boldsymbol{\varphi}}_{(n-r)i}^R(j\hat{\omega}_i,V) \\ \hat{\boldsymbol{\varphi}}_{ri}^R(j\hat{\omega}_i,V) \end{bmatrix} = \mathbf{0}.$$ (12)

Simplifying Eq. (12) leads to [28]

$$(\mathbf{I}_{rr}+\mathbf{H}_{rr}(j\hat{\omega}_i,V)\Delta\mathbf{K}_{rr})\hat{\boldsymbol{\varphi}}_{ri}^R(j\hat{\omega}_i,V) = \mathbf{0}.$$ (13)

At the same time, one can conclude that [33]

$$\det(\mathbf{I}_{rr}+\mathbf{H}_{rr}(j\hat{\omega}_i,V)\Delta\mathbf{K}_{rr}) = \mathbf{0},$$ (14)

where $\mathbf{H}_{rr}(j\hat{\omega},V)$ is an asymmetric matrix and renamed the modification-related receptance matrix consisting of the cross- and point- FRFs at all modification-related locations in the original system. Eq. (14) clearly shows that only these FRFs are required, and the ones at other locations do not need to be known.

When multiple desired natural frequencies $(\hat{\omega}_{i_1}, \hat{\omega}_{i_2}, \cdots)$ are required, this means that all of the equations in the following equation set must be true

$$\begin{cases} \det(\mathbf{I}_{rr} + \mathbf{H}_{rr}(\hat{\omega}_{i_1}, V)\Delta\mathbf{K}_{rr}) = 0 \\ \det(\mathbf{I}_{rr} + \mathbf{H}_{rr}(\hat{\omega}_{i_2}, V)\Delta\mathbf{K}_{rr}) = 0 \\ \qquad\qquad \vdots \\ \det(\mathbf{I}_{rr} + \mathbf{H}_{rr}(\hat{\omega}_{i_a}, V)\Delta\mathbf{K}_{rr}) = 0 \end{cases} \tag{15}$$

Clearly, the abovementioned equation set is difficult to solve, and so the equation-solving problem is converted into a MOP that is easier to solve, as it is suggested in Ref [26,31]. The objective-function vector of the MOP can be expressed as

$$\mathbf{\Psi} = \min\{\Psi_1, \Psi_2, \cdots \}, \tag{16}$$

where a is the number of desired natural frequencies (sub-objective) and the λth sub-objective function is the Euclidean norm of $\det(\mathbf{I}_{rr} + \mathbf{H}_{rr}(\omega_{i_\lambda}, V)\Delta\mathbf{K}_{rr})$ [26]

$$\Psi_\lambda = \left\| \det(\mathbf{I}_{rr} + \mathbf{H}_{rr}(\hat{\omega}_{i_\lambda}, V)\Delta\mathbf{K}_{rr}) \right\|_2. \tag{17}$$

For arbitrary FRF $h_{pq}(\mathrm{j}\omega, V)$ required to form $\mathbf{H}_{rr}(\hat{\omega}_{i_\lambda}, V)$, it can be measured by processing the signal of vibration excited by an impact hammer (applying hammer force to coordinate q and measuring the response of coordinate p) [48]. Therefore, neither the finite element model of the system nor complete modal testing of the structure needs to be conducted theoretically.

The to-be-determined $\Delta\mathbf{K}_{rr}$ can be obtained by using an optimization algorithm to minimize the objective-function vector $\mathbf{\Psi}$ synthetically. A mature and widely-used NSGA-II algorithm provided by MathWorks called *gamultiobj* is adopted to solve this optimization problem. Generally speaking, NSGA-II gives rise to a set of Pareto-optimal solutions instead of a single optimal solution, which allows engineers to choose the appropriate modifications according to their preferences. As far as this paper is concerned, the Pareto-optimal solutions corresponding to the minimum mean square

11

root of objective function values are selected as the required modifications. The NSGA-II algorithm is not the focus of this paper, which is why its history, developments, and essential features are not presented here. Specific details of the NSGA-II algorithm can be found in [40,49].

2.4 Interval-based natural frequency assignment method

Considering that the working condition of the industrial fluid-conveying pipeline is changeable, the flow speed of its carried fluid may not have a constant value, which will lead to the measured FRFs being different at different working conditions and having an interval characteristic [11]

$$h_{pq}(\omega, V) \in \left[\underline{h}_{pq}(\omega), \ \overline{h}_{pq}(\omega) \right]. \tag{18}$$

In which $\underline{h}_{pq}$ and $\overline{h}_{pq}$ represent the lower and upper bounds of the changeable FRF, which can be theoretically determined by the FRF at the maximum and minimum flow speeds.

$$\begin{cases} \underline{h}_{pq}(\omega) = \min(h_{pq}(\omega, V_{\min}), \ h_{pq}(\omega, V_{\max})) \\ \overline{h}_{pq}(\omega) = \max(h_{pq}(\omega, V_{\min}), \ h_{pq}(\omega, V_{\max})) \end{cases}. \tag{19}$$

Considering that the industrial pipeline has a variety of working conditions, the changeable flow speed of the carried fluid can be regarded as an uncertain parameter of the system. Given the interval characteristic of the FRF variation, the changeable FRF of the pipeline system is redefined as interval FRF by introducing the interval analysis [50,51].

$$H_{pq}(\omega, V) = \left[\underline{h}_{pq}(\omega), \ \overline{h}_{pq}(\omega) \right]. \tag{20}$$

For arbitrary circular frequency ω, the centre and width of the interval FRF can be expressed as

$$\begin{aligned} H_{pq}^{c}(\omega, V) &= \frac{\underline{h}_{pq}(\omega) + \overline{h}_{pq}(\omega)}{2} \\ H_{pq}^{w}(\omega, V) &= \frac{\overline{h}_{pq}(\omega) - \underline{h}_{pq}(\omega)}{2} \end{aligned}, \tag{21}$$

where superscripts c and w represent the midpoint and width of the interval FRF, respectively.

Similarly, the λth objective function of the natural frequency assignment in Eq. (16) can be recast as an interval form

$$\Psi_i(\hat{\omega}_{i_\lambda}, V) = \left[\underline{\Psi}_i(\hat{\omega}_{i_\lambda}), \ \overline{\Psi}_i(\hat{\omega}_{i_\lambda}) \right]. \tag{22}$$

By using the natural interval extension [37], the upper and lower bounds of the interval objective can respectively be written as

$$\begin{cases} \underline{\Psi}_i(\hat{\omega}_{i_\lambda}) = \Psi_i^c(\hat{\omega}_{i_\lambda}, V) - \displaystyle\sum_{p=p_1}^{p_r} \sum_{q=q_1}^{q_r} \left| \frac{\delta \Psi_i^c}{\delta H_{pq}^c} \right| H_{pq}^w \\[4mm] \overline{\Psi}_i(\hat{\omega}_{i_\lambda}) = \Psi_i^c(\hat{\omega}_{i_\lambda}, V) + \displaystyle\sum_{p=p_1}^{p_r} \sum_{q=q_1}^{q_r} \left| \frac{\delta \Psi_i^c}{\delta H_{pq}^c} \right| H_{pq}^w \end{cases}, \tag{23}$$

where $\Psi_i^c(\hat{\omega}_{i_\lambda}, V) = \left\| \det(\mathbf{I}_{rr} + \mathbf{H}_{rr}^c(\hat{\omega}_{i_\lambda}, V) \Delta \mathbf{K}_{rr}) \right\|_2$, in which $\mathbf{H}_{rr}^c(\hat{\omega}_{i_\lambda}, V)$ is the centre receptance matrix consisting of the centre of the interval FRFs at all modification-related locations.

It should be noted that interval numbers cannot be directly compared, which is not conducive to the evaluation of evolutionary individuals in the optimization calculation. Therefore, this paper introduces order relationships to compare interval numbers in interval number programming: for two interval numbers A and B, $A \leq B$ needs to satisfy the following conditions [39]

$$A \leq B \quad \text{if } A^c \leq B^c \text{ and } A^w \leq B^w. \tag{24}$$

Correspondingly, the minimum problem of the interval objective $\Psi_i(\hat{\omega}_{i_\lambda}, V)$ can be converted to a programming problem with two deterministic objectives as follows [39]

$$\min\{\Psi_i(\hat{\omega}_{i_\lambda}, V)\} = \min\{\Psi_i^c(\hat{\omega}_{i_\lambda}, V), \ \Psi_i^w(\hat{\omega}_{i_\lambda}, V)\} = \min\{\Psi_i^c(\hat{\omega}_{i_\lambda}, V), \ \sum_{p=p_1}^{p_r} \sum_{q=q_1}^{q_r} \left| \frac{\delta \Psi_i^c}{\delta H_{pq}^c} \right| H_{pq}^w \}. \tag{25}$$

By using the linear combination method, the two deterministic objective functions can be integrated as a new objective function [52]

$$\Gamma_i(\hat{\omega}_{i_\lambda}, V) = \chi \Psi_i^c(\hat{\omega}_{i_\lambda}, V) + (1 - \chi) \Psi_i^w(\hat{\omega}_{i_\lambda}, V) = \chi \Psi_i^c(\hat{\omega}_{i_\lambda}, V) + (1 - \chi) \sum_{p=p_1}^{p_r} \sum_{q=q_1}^{q_r} \left| \frac{\delta \Psi_i^c}{\delta H_{pq}^c} \right| H_{pq}^w, \tag{26}$$

where $0 \leq \chi \leq 1$ is a weighting factor that can be chosen appropriately based on the practical problem and the experience of the designer.

When multiple natural frequencies need to be assigned, Eq. (16) can be recast as

$$\Gamma=\min\{\Gamma_1, \Gamma_2, \cdots \qquad . \tag{27}$$

It should be stressed that the first term of Eq. (27) is used to control the assignment accuracy of the natural frequency, while the second term is used to control the perturbation range of the assigned natural frequency. By choosing a reasonable weight factor and minimizing the objective-function vector Ψ synthetically, the optimal stiffness modifications of the elastic supports are obtained and can be used to solve the two problems in Section 2.1.

3. The experimental model for the fluid-conveying pipeline system

3.1 Test setup

The experimental setup shown in Fig. 1 is a U-shaped pipeline (marked by a solid red line). The two ends of the pipeline are clamped to a very rigid cast iron test bench, and the supports in the middle are five shock absorbers of the same type. The outer diameter and thickness of the pipeline are 32 and 1.5 mm, respectively. The pipeline is made from 304L stainless steel with a Young's modulus value of 196 GPa and a density of 7850 kg/m^3. Each shock absorber is composed of a housing and an inner spring (this structural type is similar to that of commercial shock absorbers); the housing is an approximately rigid body with a weight of 0.47 kg, and the inner spring is an elastic element with an axial stiffness of 22 kN/m.

The carried fluid is common freshwater with a density of 1000 kg/m^3. According to previous research [2,35,36,53], the effect of one-way FSI on the lateral dynamic behaviour of the pipeline system is mainly reflected in the mass and flow speed of the carried water. Therefore, this paper places emphasis on the impact of mass and flow speed on the natural

frequency of the fluid-conveying pipeline (the flow direction of the carried water is marked by a blue arrow in Fig. 1). In each test, the flow of the carried water is monitored by the flowmeter on the pipeline, and the corresponding flow speed can be calculated based on the flow-monitor value and section dimensions of the pipeline.
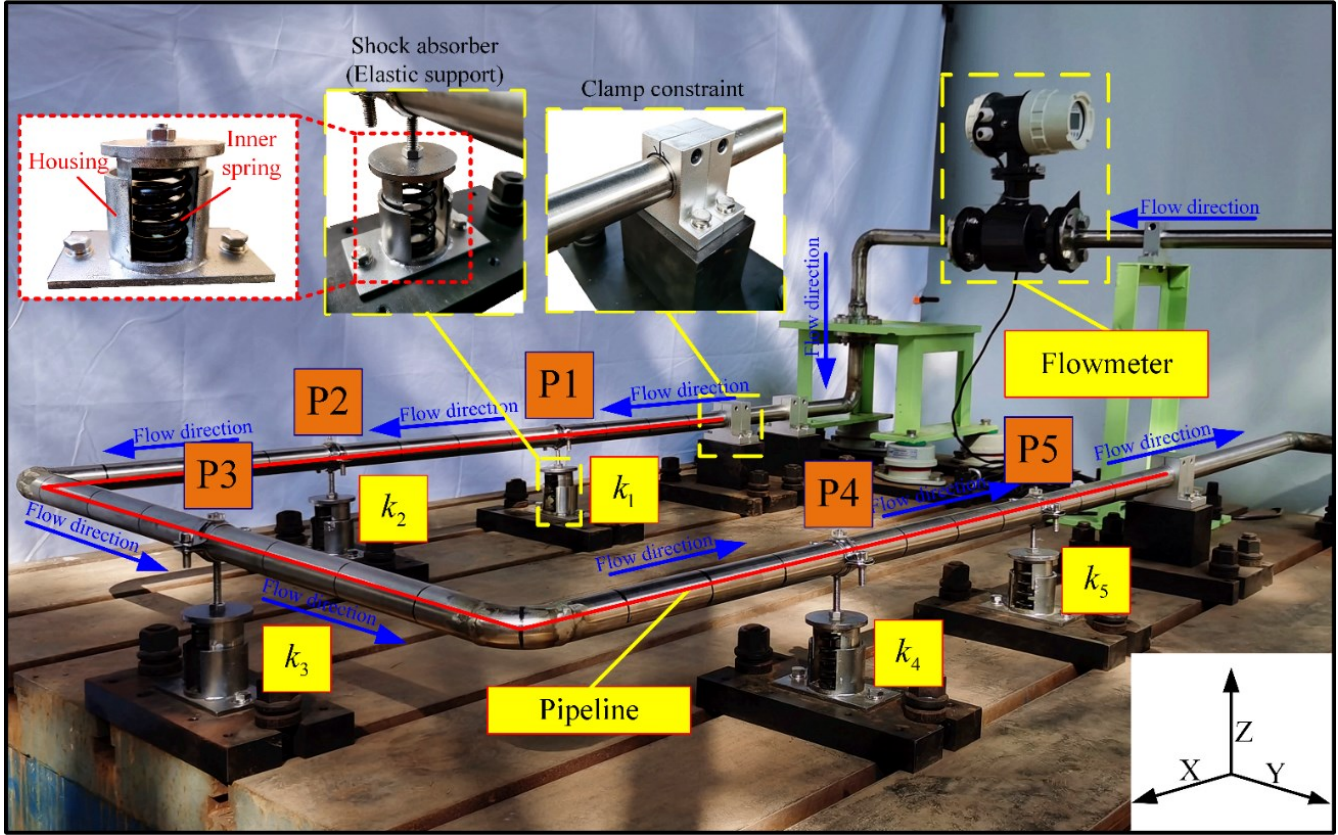

Fig. 1. The experimental model for the fluid-conveying pipeline system.

Schematics of the control and related pieces of the fluid-flow equipment are displayed in Fig. 2. In this study, the flow speed of the carried water (V) mainly depends on the initial pressure in the pressure vessel. Before each test, the water in the reservoir is injected into the pressure vessel via a high-pressure water pump, and the water delivery is stopped until the pressure gauge reaches the set initial pressure. Subsequently, the inlet and outlet water valves are opened simultaneously, and the impact hammer test is performed. It should be noted that the water pump is turned off during the impact hammer test so that the measured FRFs are only excited by the impact hammer and not by the water pump.
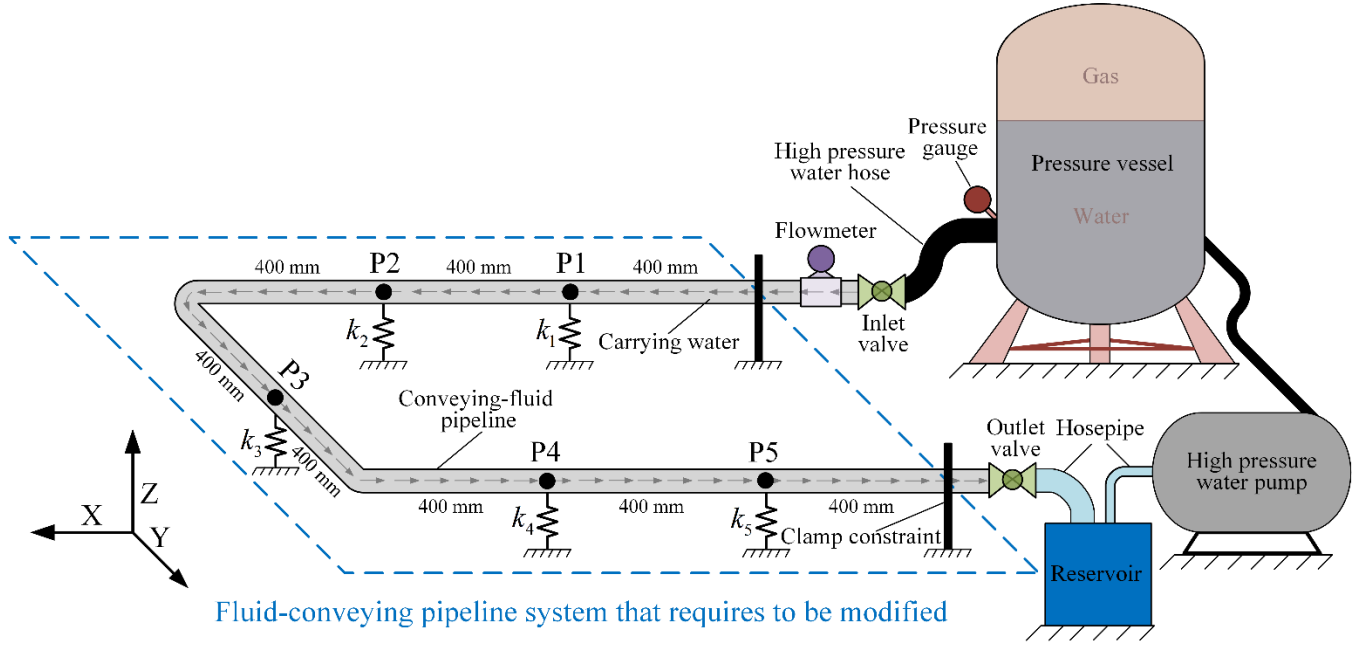
Fig. 2. A schematic of the pipeline system.

Four different working conditions (the corresponding flow velocity is 0.0, 3.7, 6.5, and 8.9 m/s, respectively) are considered (the initial pressures corresponding to the three flow states $(V \neq 0)$ are 2.1, 2.8, and 3.5 MPa). It should be noted that the flow speed of the carried water cannot be calculated directly by using Bernoulli's equation since the frictional head loss of the carried water is very large when flowing past the high-pressure water hose [2].

In practice, the direction of the excitation source is generally the same as the pipeline's installation direction (the Z-direction in this study). As far as this structure is concerned, the Z-direction vibration of the pipeline is not theoretically coupled with X- and Y-directional vibrations. Thus, the Z-direction vibration of the pipeline is only related to the Z-direction stiffness of the elastic supports and is not affected by its X- and Y- direction stiffness. Considering the abovementioned factors, the Z-direction stiffness of the shock absorber is required to modify to assign the pipeline system's Z-direction natural frequency. The Z-direction stiffness of the shock absorber can be changed by replacing its inner spring. The five shock absorbers are denoted as k_1 to k_5, as shown in Fig. 2.

A total of five measurement points (P1 to P5) are set along the pipeline, as shown in Figs. 2 and 3. The Z-coordinate

16

of each measuring point is the same as that of one of the shock absorber installation locations; for example, the Z-coordinate of P1 is the same as that of k_1. The point and cross FRFs of P1–P5 are measured via impact hammer tests (employing the impact hammer as the excitation mechanism and the accelerometer as the response monitoring sensor) [48]. Before each impact hammer test, five Donghua miniature accelerometers (Model 1A116E) weighing 6.62 g each are used to monitor accelerations at the measurement points and simultaneously minimize the mass-loading effect. The impact hammer is an LC02 impact hammer (Model 3A102) with a plastic hammer tip. Signals are sampled through a DH5902 signal acquisition system (capable of transferring test data to a PC in real-time) at a sampling rate of 2.56 kHz. DHDAS software is used for signal processing and modal parameter estimation, after which the measured FRFs are exported directly from the DHDAS software.

3.2 Theoretical model of the U-shaped pipeline system

The theoretical dynamic model of the experimental U-shaped pipeline system is established by using Eq. (1-3) and solved by using Zhang et al.'s method [2], and then a semi-analytical solution for the FRFs of the U-shaped pipeline system can be obtained. It should be noted that the theoretical dynamic model does not play a direct role but is only used to assist in demonstrating the proposed method, and the natural frequency assignment of real pipelines can be done entirely using measured receptances (FRFs).

The physical parameters of the theoretical model quantitatively well represent those for the test model in Section 2.1. The shock absorber is simulated as a spring with a stiffness of 22 kN/m and a point mass with a weight of 0.157 kg (one-third of the housing weight), whose values are measured.

3.3 Dynamic performance of fluid-conveying pipeline systems at various flow speeds

In this study, symbol *h* is used to represent the FRFs and h_{pZqZ} is the Z-direction harmonic response at coordinate *p* caused by a single Z-direction unit harmonic force applied to coordinate *q* [48]. For example, h_{1Z1Z} represents the point

FRF of measured point P1, which is the Z-direction frequency response of P1 caused by the Z-direction hammer force applied to P1; h_{2Z3Z} represents the cross FRF of measured point P3 to P2, the Z-direction frequency response of P2 caused by the Z-direction hammer force applied to P3.

Fig. 3a displays the magnitudes of experimental point FRFs h_{1Z1Z} at the four different flow speeds; the frequency range of interest is limited to below 120 Hz, which covers the first four modes of the fluid-conveying pipeline. The first four natural frequencies are identified by using the peak picking method and recorded in Table 1 [54].

The modal analyses of the theoretical model are carried out, and its natural frequencies at the four flow speeds used in the tests are also collected in Table 1. By comparing with the experimental results, the dynamic behaviours of the experimental pipeline are effectively explained and the assumptions about the theoretical model are demonstrated.
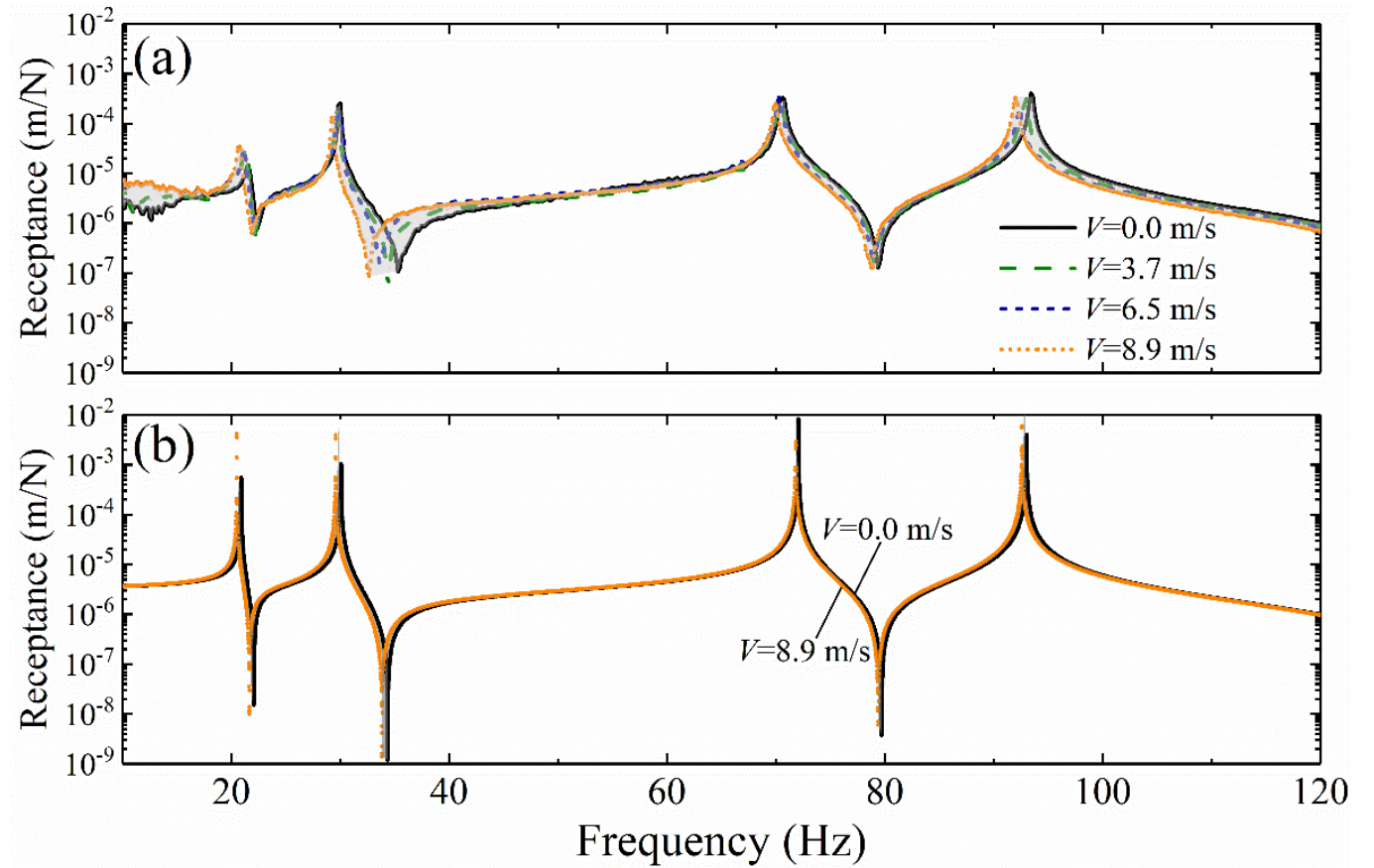

Fig. 3. The point FRFs of P1 in the Z-direction h_{1Z1Z} : (a) experimental result; (b) numerical results.

Table 1. Natural frequencies of the fluid-conveying pipeline system.

		Natural frequency (Hz)			
		V=0.0 m/s (static)	V=3.7 m/s	V=6.5 m/s	V=8.9 m/s
Mode 1	Experimental	21.56	21.35	21.15	20.89
	Numerical	20.93	20.75	20.63	20.50
Mode 2	Experimental	30.08	29.74	29.55	29.43
	Numerical	30.08	29.91	29.75	29.58
Mode 3	Experimental	70.63	70.47	70.31	70.08
	Numerical	72.08	72.00	71.92	71.78
Mode 4	Experimental	93.44	93.12	92.63	92.33
	Numerical	93.02	92.87	92.75	92.63

It is clear from Fig. 3 and Table 1 that the experimental results are in good agreement with the numerical results. However, it is necessary to explain the error between the numerical results, compared with the experimental ones. The modelling error mainly lies in the numerical model's system parameters. This error is primarily caused by the inaccurate representation of the boundaries of the experimental model in the theoretical model [55]. However, such an error is not important in this paper, since the main purpose of the theoretical model is to assist in verifying the rationality of the simplified treatment of the FSI effect and the effectiveness of the receptance method. It is unnecessary to spend much time in tuning the numerical model to fit the test data, since the natural frequency assignment of the experimental fluid-conveying pipeline is only based on the measured FRFs (receptances), not the numerical FRFs. Therefore, this paper only requires the theoretical model to have dynamic characteristics approximate to the test one.

Moreover, it should be noted in Fig. 3 that the FSI has only a marginal impact on the system's natural frequencies and can be regarded as a kind of perturbation. Such perturbation renders the FRFs(receptance) at the non-resonance zone becoming an interval-uncertain form [11].
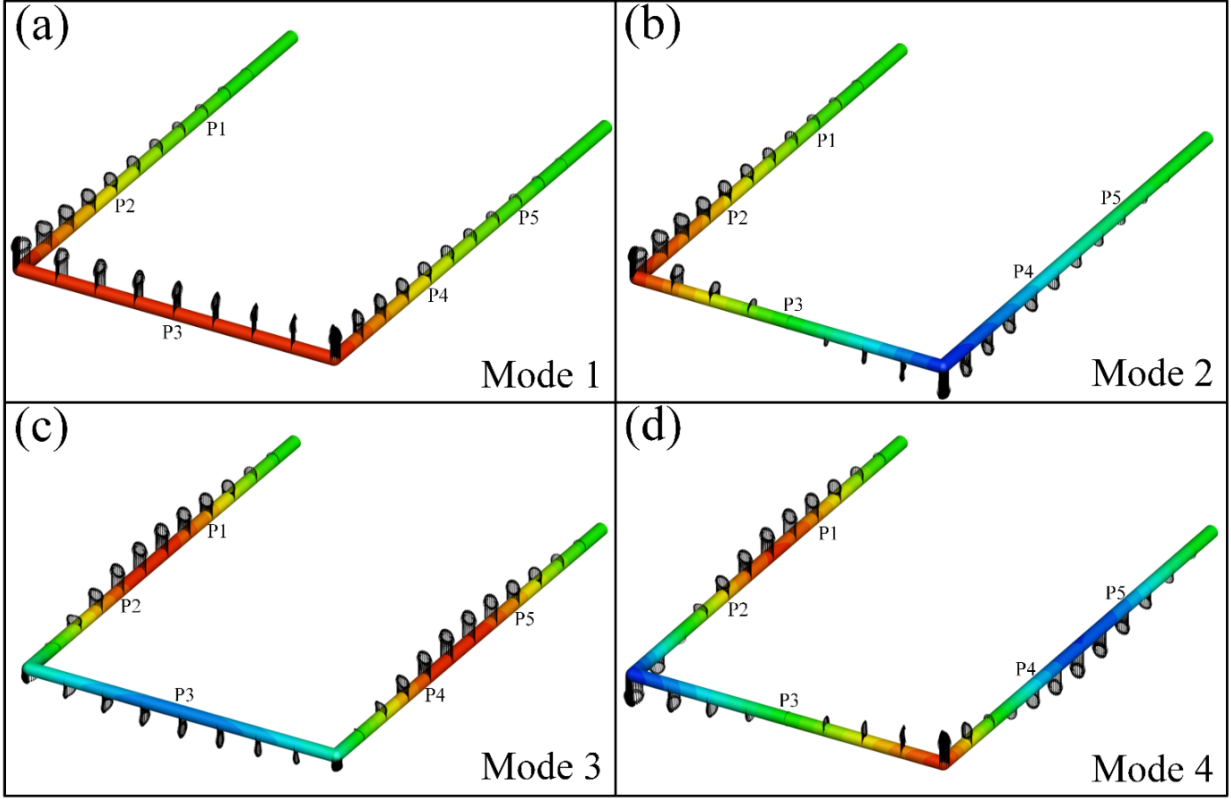
Fig. 4. The shapes of the first four modes at the static state.

Fig. 4 displays the mode shapes of the first four natural frequencies in the static fluid state ($V = 0$ m/s). It should be highlighted that the eigenvectors of the fluid-conveying pipeline in the static fluid state are real vectors, whereas those in the flow state are complex vectors. It should be noted that the skew-symmetry of the fluid damping matrix means that the left eigenvectors of the pipeline system $\boldsymbol{\varphi}_i^L$ are equal to the conjugate transpose of the corresponding right eigenvectors $\boldsymbol{\varphi}_i^R$ when the system is in the flow state [36].

4. Natural frequency assignment of the fluid-conveying pipeline with a constant flow speed

The interval-based natural frequency assignment method is based on the framework of the receptance method, and so it is necessary to verify the effectiveness of the receptance method. The verification work of the receptance method is carried out on the pipeline system with a constant flow speed, which is a deterministic linear system.

4.1 Numerical validation of receptance method

In order to make the verification more reliable, the receptance-based natural frequency assignment is firstly achieved on the theoretical model of the pipeline system. It should be stressed again that the numerical validation is just used to check the effectiveness of the receptance method, and the subsequent natural frequency assignment of the experimental pipeline system is entirely based on the measured receptance (FRFs) and not on the numerical ones [22].

In the present example, the higher-rank structural modification is conducted, in which the second and third natural frequencies of the system are assigned simultaneously. In order to avoid the loss of generality, the minimum and maximum flow speeds in tests, 0 m/s and 8.9 m/s, are considered. The desired frequencies are assumed as 40 Hz and 80 Hz. The FRFs of the modification-related locations P1-P5 of the theoretical model are obtained by a series of harmonic analyses, and then the required receptance matrices are constructed. It should be stressed that the cross FRF $h_{pq} \neq h_{qp}$ at V=8.9 m/s since the fluid-conveying pipeline at a flow state is an asymmetric system.

For each flow speed scenario, Eq. (16) is used to establish the objective functions, and the NSGA-II algorithm is employed to search for the corresponding optimal solutions (modifications), as shown in Table 2. It should be noted that the feasible domain for all of the optimal solutions (modifications) is set as [−22, 200] kN/m to ensure that the calculated results have physical implications.

Table 2. A summary of the stiffness modifications.

Flow speed	Stiffness modification				
	Δk_1 (kN/m)	Δk_2 (kN/m)	Δk_3 (kN/m)	Δk_4 (kN/m)	Δk_5 (kN/m)
V=0 m/s	30.33	0.63	150.74	25.01	-0.86
V=8.9 m/s	33.55	5.46	148.86	24.65	2.33

The two sets of stiffness modifications in Table 2 are applied to the pipeline system with fluid flow speeds of 0 m/s and 8.9 m/s respectively, and then the FRFs of the modified system h_{1Z1Z} are obtained by harmonic analysis and shown in Fig. 5. The first four natural frequencies of the modified system are calculated by modal analysis and shown in Table

3. For each flow speed scenario presented previously, the natural frequencies of the modified system have been shifted exactly at the desired location, which proves the effectiveness of the receptance method.
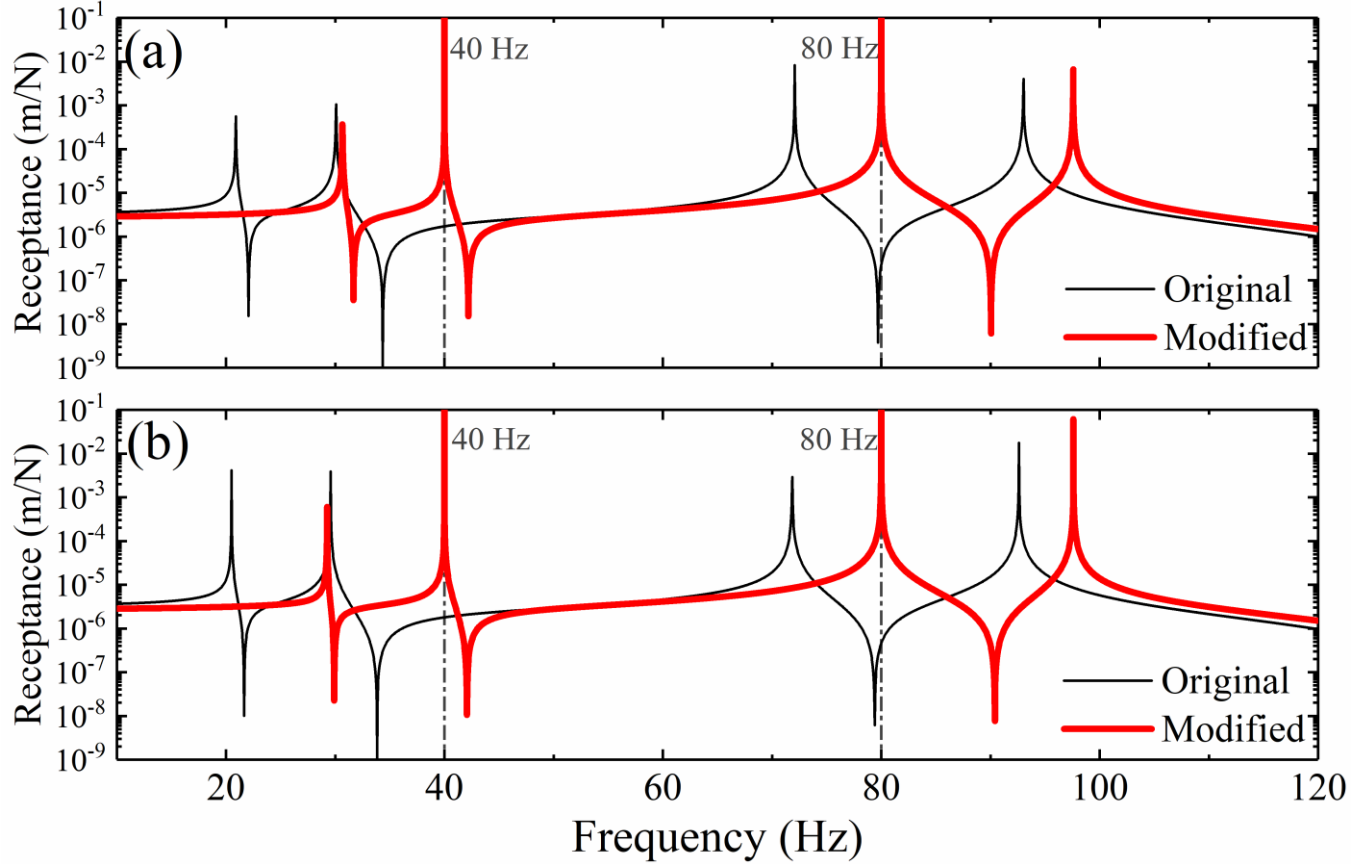

Fig. 5. The point FRFs of P1 in the Z-direction h_{1Z1Z} before and after modification: (a) V=0 m/s; (b) V=8.9 m/s.

Table 3 The first four natural frequencies of the fluid-conveying pipeline system before and after modification.

		Mode 1	Mode 2	Mode 3	Mode 4
V=0 m/s	Original	20.93 Hz	30.08 Hz	72.08 Hz	93.02 Hz
	Modified	30.65 Hz	**40.00 Hz**	**80.00 Hz**	97.58 Hz
V=8.9 m/s	Original	20.50 Hz	29.58 Hz	71.78 Hz	92.63 Hz
	Modified	29.25 Hz	**40.00 Hz**	**80.00 Hz**	97.60 Hz

Moreover, it should be highlighted that the required stiffness modifications at V=8.9 m/s have slight differences from those at V=0 m/s. Such minor differences are impossible to be considered when implementing stiffness modification in real due to the machining error of the elastic element (such as spring) [56]. Moreover, those tiny difference indicates

that the influence of FSI on structural modification calculation is marginal. Once again, it is reasonable to regard the changeable flow speed as an interval uncertainty when the carried water of the pipeline system is in a low flow state.

4.2 Natural frequency assignment of the experimental pipeline system

This section aims to realize the natural frequency assignment of 40 Hz and 80 Hz for the experimental pipeline system in section 3.1 and demonstrate the working of the receptance method from a profound perspective. Due to the similarity of the structural modification at different flow speeds and the difficulty of the physical implementation of precise modifications, the receptance-based natural frequency assignment is realized only on the experimental pipeline system with a flow speed of V=8.9 m/s. In the present example, the calculation of the structural modification is entirely based on the measured receptance. The relevant settings for optimization calculation are the same as in Section 4.1, and the obtained optimal modifications are shown in the third column of Table 4.

Table 4. the stiffness modifications obtained by measured receptance.

Stiffness modification (kN/m)	Δk_1	Δk_2	Δk_3	Δk_4	Δk_5
The calculated	25.09	8.21	156.50	-2.56	11.73
The real	26.31	7.44	161.28	0	15.45
Difference	+1.22 (4.87%)	-0.77 (9.38%)	+4.78 (3.05%)	+2.56 (100%)	+3.72 (31.71%)

The required stiffness ($\hat{k}_i = k_i + \Delta k_i$) of the inner spring for realizing the natural frequency assignment is calculated by using the stiffness modifications in Table 4, after which the structural modification could be implemented physically. The specific modification process is as follows

(**i**) Design and manufacture new inner springs $\hat{k}_1 - \hat{k}_5$ with the designated stiffness based on the standards for cylindrical spiral springs [57] (Fig. 6a).

(**ii**) Measure the real stiffness of the new springs on a compression tester (Fig. 6b) and record the real stiffness modifications (the fourth column in Table 4). The stiffness of the designed springs needs only be approximately equal

to the target stiffness due to several restrictive factors.

(iii) Replace the original inner spring in each shock absorber with the designed spring.

(iv) Reinstall the shock absorbers in the pipeline system and conduct a series of impact hammer tests to measure the FRFs of the modified pipeline system.
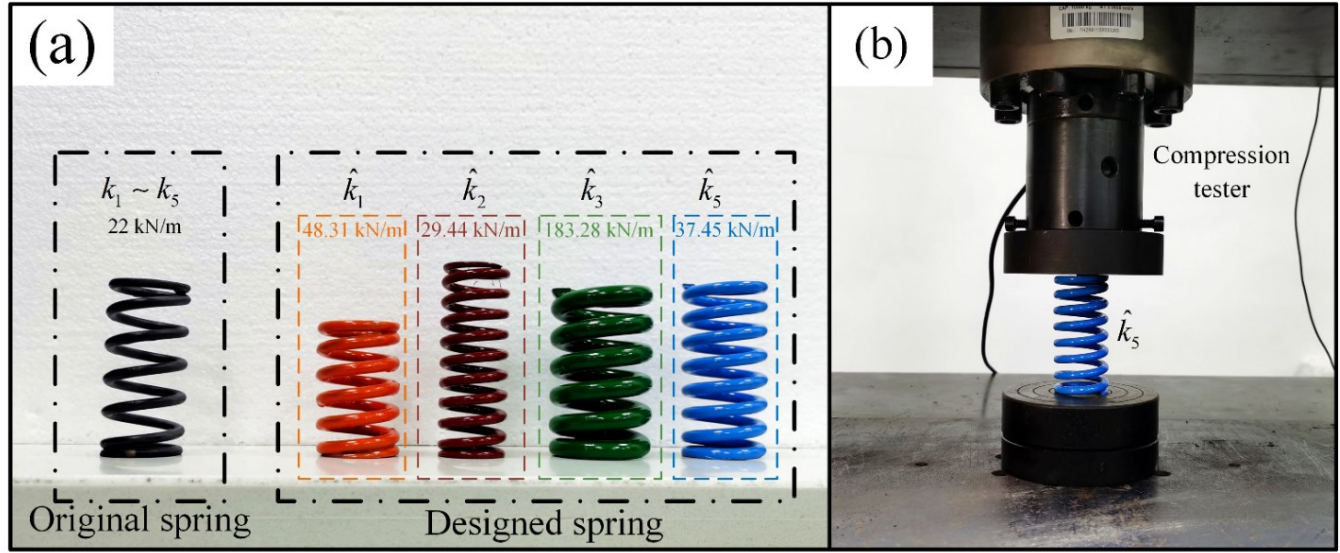

Fig. 6. The inner spring design and stiffness testing. (a) the original and designed springs and (b) stiffness testing of the spring.

The desired natural frequencies of the pipeline system are assigned after executing the above procedure. Fig. 7 shows the experimental values of FRF h_{1Z1Z} before and after modification. Subsequently, the natural frequencies of the modified pipeline system are estimated by applying the peak picking method, the results of which are presented in Table 5.

Fig. 7 and Table 5 clearly show that the assigned natural frequencies of the pipeline system are very close to the desired frequencies even though there is a certain error between the real modifications and the calculated ones. Such an accurate structural modification demonstrates the rationality of the experimental implementation procedure, which provides a reasonable and reliable approach for the structural modification of the fluid-conveying pipeline system.

In order to evaluate the receptance method comprehensively, the experimental results are compared with the

numerical ones, and the consistencies between the two are checked. Comparison results show that (**i**) the stiffness modifications obtained by numerical receptance and those obtained by measured receptance are similar; (**ii**) the modified first four natural frequencies of the theoretical and experimental models are approximately equal, and the maximum error is not even more than 2 Hz. This fact also provides solid evidence of the rationality of those assumptions about the theoretical model in Section 2.1. This investigation improves the confidence in realizing the natural frequency assignment of a fluid-conveying pipeline by using the receptance method.
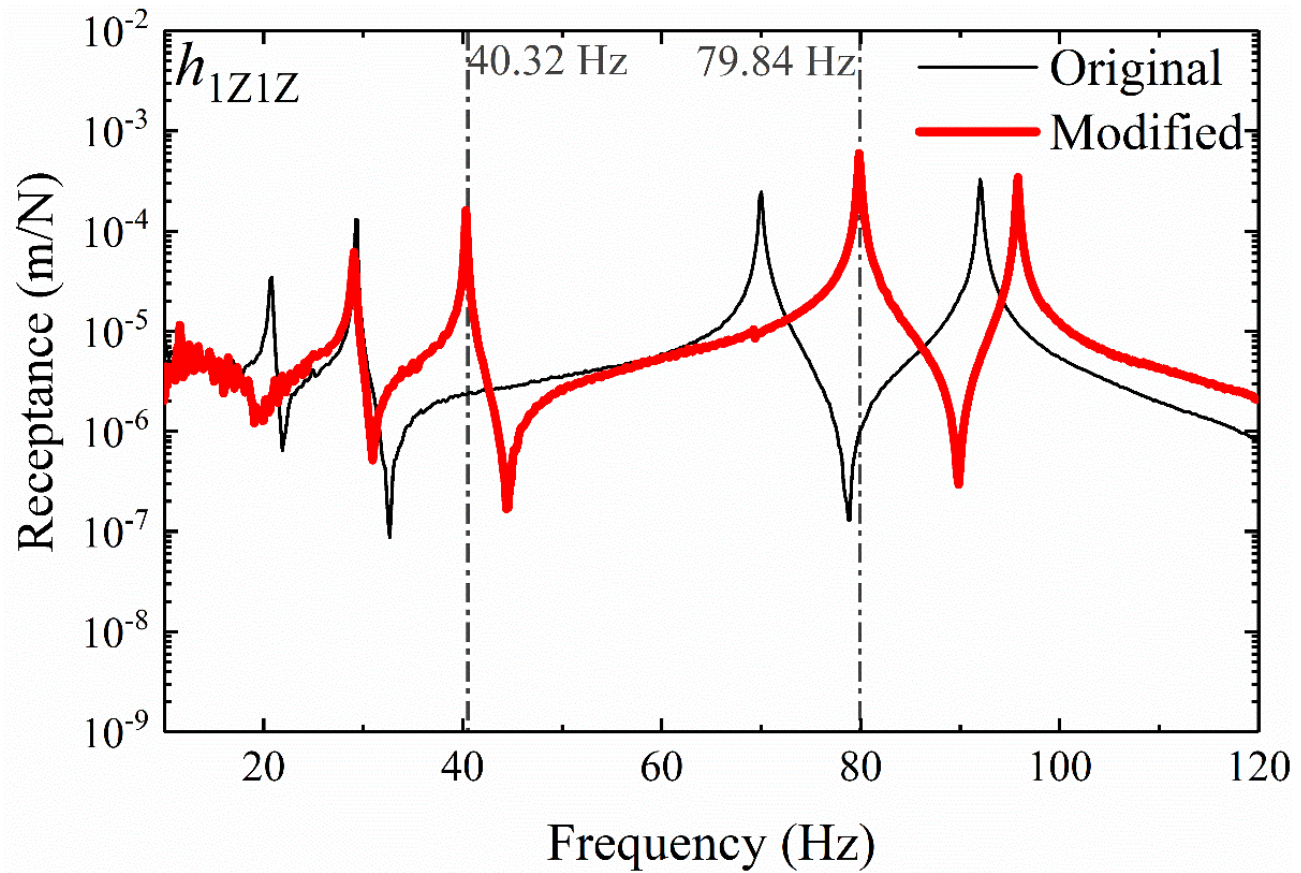

Fig. 7. FRF h_{1Z1Z} of the pipeline system before and after modification when flow speed is 8.9 m/s.

Table 5. The first four natural frequencies of the fluid-conveying pipeline system before and after modification.

	Mode 1	Mode 2	Mode 3	Mode 4
Before modification	21.09 Hz	29.53 Hz	70.08 Hz	92.43 Hz
After modification	29.06 Hz	**40.32** Hz (0.78%)	**79.84** Hz (-0.21%)	95.78 Hz

5. Natural frequency assignment to the fluid-conveying pipeline with an uncertain flow speed

5.1 Numerical verification of interval-based natural frequency assignment method

In order to assess the effectiveness of the interval-based natural frequency assignment method numerically, it has been firstly applied to the structural modification of the pipeline system with changeable working conditions. It is assumed that the flow speed of the carried water in the pipeline varies from 0 m/s to 8.9 m/s and the desired natural frequencies are 35 Hz and 80 Hz. Clearly, the uncertain flow speed will lead to the FRFs of the pipeline system becoming interval–uncertain functions and the natural frequencies becoming interval-uncertain values [11,36]. In order to analyse the effect of the weighting factor χ on the working of the interval-based natural frequency assignment method, four values of this weighting factor are considered, and the corresponding stiffness modification schemes are determined using Eq. (27) and shown in Table 6.

Table 6. Stiffness modification scheme at the four values of the weighting factor

	Weighting factor	Δk_1 (kN/m)	Δk_2 (kN/m)	Δk_3 (kN/m)	Δk_4 (kN/m)	Δk_5 (kN/m)
Scheme 1	χ=0.25	-0.14	88.61	47.88	87.19	-3.46
Scheme 2	χ=0.5	-14.44	61.60	58.65	60.66	-3.45
Scheme 3	χ=0.75	29.89	65.38	82.54	33.42	34.90
Scheme 4	χ=1	27.66	45.09	110.34	32.19	29.41

By implementing the four modification schemes, the interval FRFs of the modified system are obtained and shown in Fig. 8. Clearly, the first and third natural frequencies of the modified system in the four schemes are gathered around 35 Hz and 80 Hz, respectively. However, the intervals of the assigned natural frequencies in the four schemes have a significant difference. In order to display such a difference clearly, the midpoint and width of the natural frequency interval and the perturbation error (whose definition is given in Eq. (28)) are employed, and the merits and demerits of

all modification schemes are evaluated.

$$E_s = \frac{\max\left\{\left|\hat{\omega}_{i_\lambda} - \underline{\omega}_{i_\lambda}^a\right|, \left|\hat{\omega}_{i_\lambda} - \overline{\omega}_{i_\lambda}^a\right|\right\}}{\hat{\omega}_{i_\lambda}} \times 100\%, \qquad (28)$$

where $\hat{\omega}_{i_\lambda}$ is the λth desired natural frequency; $\underline{\omega}_{i_\lambda}^a$ and $\overline{\omega}_{i_\lambda}^a$ represents the lower and upper bounds of the perturbation

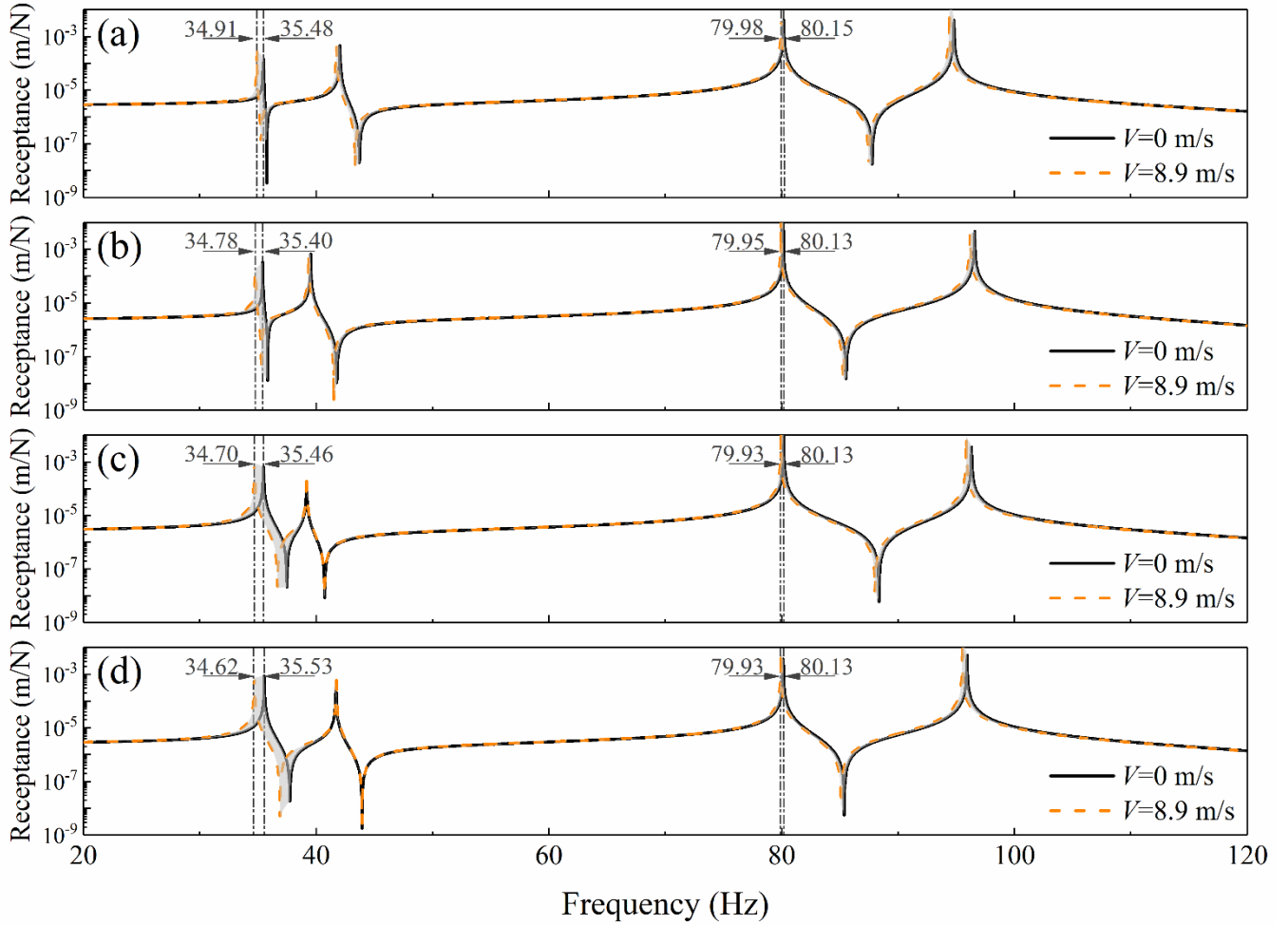interval of the λth assigned natural frequency, respectively.

Fig. 8. The point FRFs of P1 in the Z-direction h_{1Z1Z} of the modified pipeline system with an uncertain flow speed: (a) χ=0.25; (b) χ=0.5;

(c) χ=0.75; (d) χ=1.

It can be easily found from Table 7 that the obtained stiffness modification scheme with a greater χ can make the

center frequency of the assigned interval natural frequency closer to the desired frequency and thus more accurate, but

the interval of the assigned natural frequency wider and thus less robust. This fact indicates that there is a clash between accuracy and the robustness in frequency assignment with interval uncertainty, and selecting a too large or small weighting factor will increase the perturbation error of the assigned natural frequency. Therefore, the weighting factor should be chosen appropriately to balance the robustness and accuracy requirements in frequency assignment and minimize the perturbation error. As far as the four cases are concerned, the weighting factor χ should be set to about 0.5 according to the magnitude of the perturbation error in Table 6.

Table 7. Results of the natural frequency assignment.

		Scheme 1	Scheme 2	Scheme 3	Scheme 4
Weighting factor		χ=0.25	χ=0.50	χ=0.75	χ=1.00
Mode 1	Frequency interval	[34.92, 35.48] Hz	[34.78, 35.40] Hz	[34.70 35.46] Hz	[34.62, 35.53] Hz
	Centre frequency	35.20 Hz	35.09 Hz	35.08 Hz	35.08 Hz
	Interval width	0.56 Hz	0.62Hz	0.76 Hz	0.91 Hz
	Perturbation error	1.37%	1.14%	1.31%	1.51%
Mode 3	Frequency interval	[79.98, 80.15] Hz	[79.95, 80.13] Hz	[79.93, 80.13] Hz	[79.93, 80.13] Hz
	Centre frequency	80.06 Hz	80.04 Hz	80.03 Hz	80.03 Hz
	Interval width	0.17 Hz	0.18 Hz	0.20 Hz	0.20 Hz
	Perturbation error	0.17%	0.16%	0.16%	0.16%

By comparing and analysing the four cases, the effectiveness of the proposed interval-based frequency assignment method has been demonstrated.

5.2 Natural frequency assignment of the experimental pipeline with an uncertain flow speed

As stated previously, the uncertain flow speed will lead to the FRFs of the pipeline system becoming interval-uncertain functions [36]. Fig. 9 displays the measured interval FRFs in the Z-direction of all the modification-related locations (P1-P5), where the maximum and minimum flow speeds are 8.9 and 0 m/s, respectively.

The desired frequencies in this section are the same as those in Section 5.1, 35 Hz and 80 Hz. The measured interval

FRFs at the two desired frequencies are extracted from Fig. 9 and substituted in Eq. (27) to calculate the optimal stiffness modifications. The obtained experimental stiffness modification schemes are shown in Table 8. Two weighting factors, the best and worst ones (χ=0.5 and χ=1) in Section 5.1, are considered in this section.
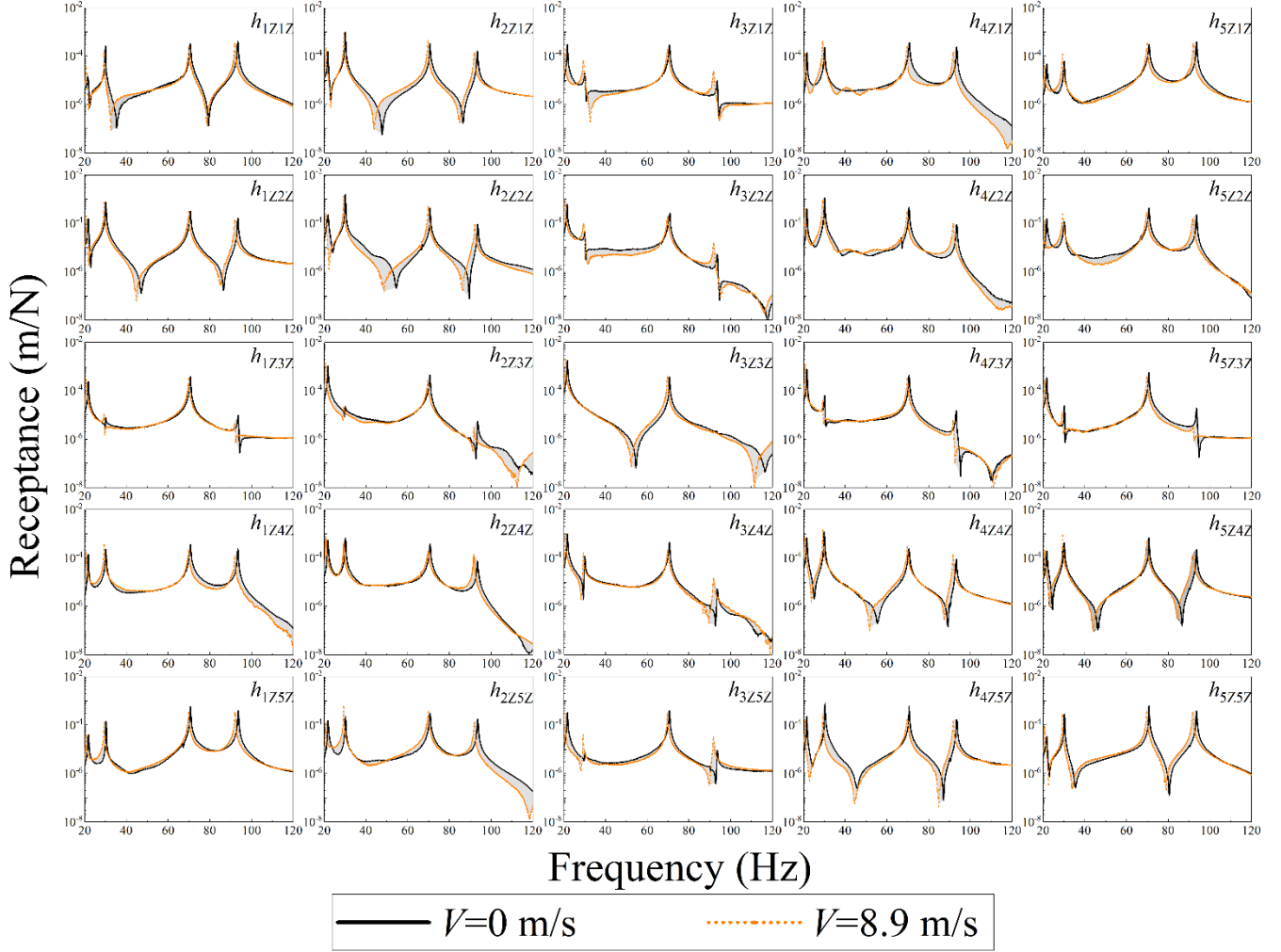

Fig. 9. Measured interval FRFs in the Z-direction of all the modification-related locations.

Table 8. Experimental stiffness modifications.

		Combination 1 (χ=0.5)			Combination 2 (χ=1)		
		The calculated	The used	Difference	The calculated	The used	Difference
Stiffness	Δk_1	-22.00	-22.00	+0.00 (0.00%)	-22.00	-22.00	+0.00 (0.00%)
modification	Δk_2	101.49	107.34	+5.85 (5.76%)	68.77	70.41	+1.64 (2.38%)

29

(kN/m)	Δk_3	81.31	79.57	-1.74 (2.14%)	135.82	127.11	-8.71 (6.41%)
	Δk_4	63.04	61.60	-1.44 (2.28%)	67.78	71.60	+3.82 (5.64%)
	Δk_5	-10.24	-8.96	+1.28 (12.5%)	34.65	30.58	-4.07 (11.75%)

By implementing the structural modification procedure described in Section 4.2, the two desired natural frequencies are assigned to the experimental fluid-conveying pipeline system. The interval FRF h_{1Z1Z} of the modified system pipeline with the uncertain flow speed is measured by using the impact hammer test, the result of which is displayed in Fig. 10. Subsequently, the interval natural frequencies after modification are estimated through peak picking and recorded in Table 9.
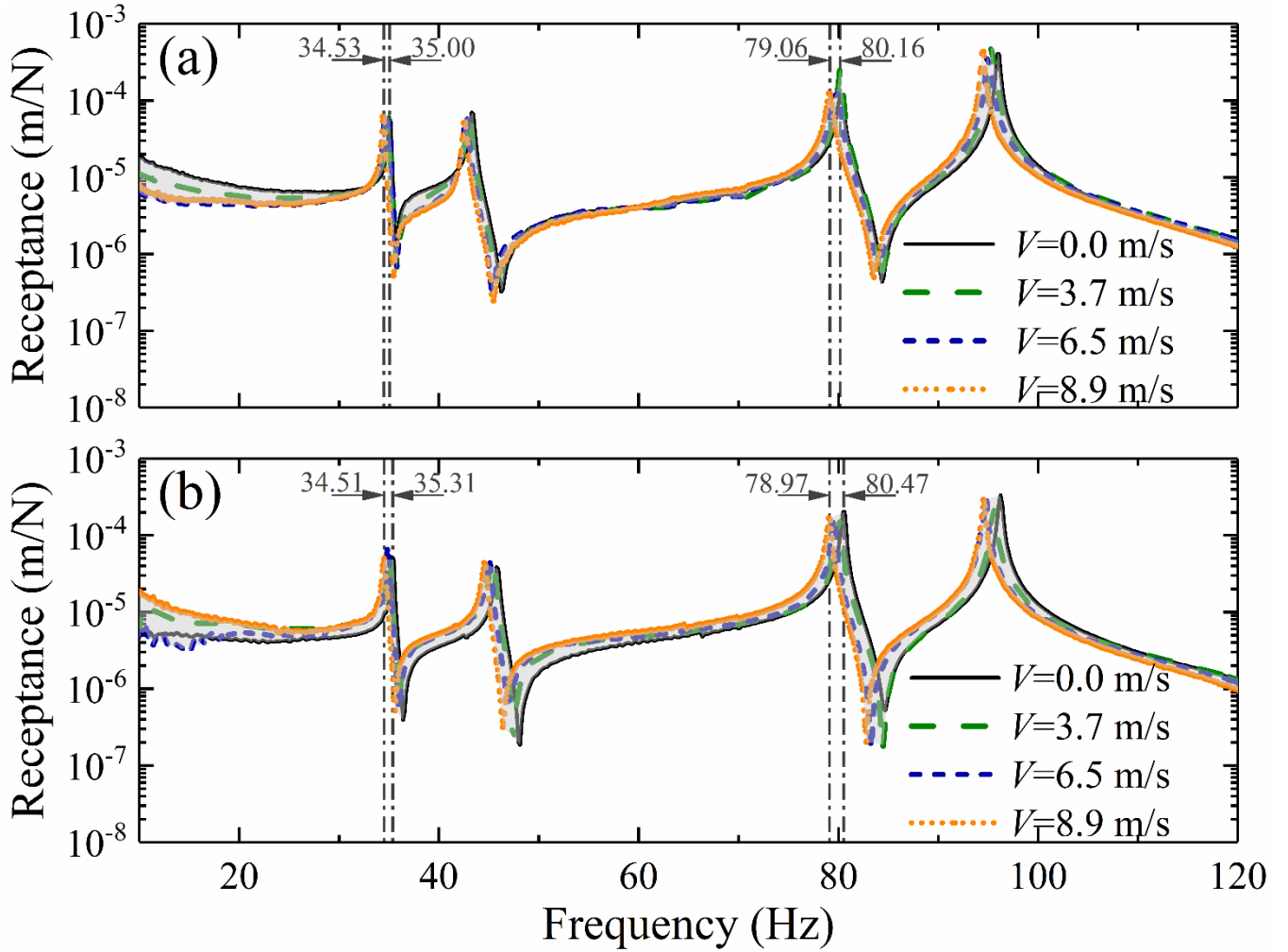

Fig. 10. Interval FRF h_{1Z1Z} values of the modified pipeline system with the uncertain flow speed: (a) Combination 1; (b) Combination 2.

It is clear from Fig. 10 and Table 9 that the two desired natural frequencies of the fluid-conveying pipeline are all successfully assigned at the two stiffness modification schemes, as is expected. More importantly, the assigned natural frequencies by using Combination 1 have higher robustness to the uncertain flow speed and smaller perturbation error than those by using Combination 2. Such a result is in good with that obtained by the numerical model in Section 5.2 and experimentally proves the effectiveness of the proposed interval-based natural frequency in Section 2.4.

Table 9. Natural frequencies of the experimental fluid-conveying pipeline system after modification.

		Frequency interval	Centre frequency	Interval width	Perturbation error
Combination 1	Mode 1	[34.53, 35.00] Hz	34.77 Hz	0.47 Hz	1.34%
(χ=0.5)	Mode 3	[79.06, 80.16] Hz	79.61 Hz	1.10 Hz	1.18%
Combination 2	Mode 1	[34.51, 35.31] Hz	34.91 Hz	0.80 Hz	1.40%
(χ=1)	Mode 3	[78.97, 80.47] Hz	80.03 Hz	1.50 Hz	1.29%

6. Conclusions

An enhanced receptance-based method for assigning higher-rank natural frequencies for a fluid-conveying pipeline system is proposed and verified experimentally. Determining the necessary modifications did not involve numerical models of the pipeline system, and only a small number of measured receptance values (FRFs) are required instead. By using a reliable implementation procedure, the structural modification of the pipeline system is firstly realized in reality. The errors between the assigned and desired natural frequencies for the pipeline system are no more than 2.5%, thereby confirming that the proposed method can accurately realize the natural frequency assignment of the fluid-conveying pipeline system, even considering the FSI effect in the steady flow state. The proposed method can help overcome the difficulties in the traditional modelling approaches and calculations for fluid-conveying pipeline optimization.

Focuses on the fluid-conveying pipeline system with an uncertain flow speed, this study extends the theory of receptance method and proposes an interval-based natural frequency assignment method. In this method, the changeable

flow speed as a feature of real working conditions is viewed as a kind of uncertainty of the system, and the concept of the interval is used to describe the effect of such uncertainty on the FRF. The accuracy of the natural frequency assignment and the robustness to the uncertain flow speed of the results are considered simultaneously, when finding the optimal stiffness modification. The numerical and experimental evidence of the effectiveness of the proposed method is provided. The structural modifications determined using this method are found to be very good in the sense that the assigned natural frequencies with a low error and high robustness are achieved.

Author Contributions

Lin Zhang: Experimental, Methodology, Formal analysis, Investigation, Visualization, Software, Writing - original draft. **Tao Zhang:** Investigation, Software, Funding acquisition, Resources, Writing - review & editing. **Huajiang Ouyang:** Conceptualization, Methodology, Formal analysis, Validation, Writing - review & editing. **Tianyun Li:** Conceptualization, Validation, Funding acquisition. **Shike Zhang:** Validation, Writing - review & editing.

Acknowledgments

Conflict of interest

We declare that we do not have any commercial or associative interest that represents a conflict of interest connected with the work submitted.

References

[1]   X. Guo, H. Ma, X. Zhang, Z. Ye, Q. Fu, Z. Liu, Q. Han, Uncertain frequency responses of clamp-pipeline systems using an interval-based method. Ieee Access, 8 (2020) 29370-29384.

[2]   T. Zhang, H. Ouyang, C. Zhao, Y.J. Ding, Vibration analysis of a complex fluid-conveying piping system with general boundary conditions using the receptance method. International Journal of Pressure Vessels and Piping, 166 (2018) 84-93.

[3]   U. Lee, J. Park, Spectral element modelling and analysis of a pipeline conveying internal unsteady fluid. Journal of Fluids and Structures, 22 (2) (2006) 273-292.

[4]   P. Gao, T. Yu, Y. Zhang, J. Wang, J. Zhai, Vibration analysis and control technologies of hydraulic pipeline system in aircraft: A review. Chinese Journal of Aeronautics, 34 (4) (2021) 83-114.

[5]   Q. Guo, Y. Liu, Y. Zhao, B. Li, Q. Yao, Improved resonance reliability and global sensitivity analysis of multi-span pipes conveying fluid based on active learning Kriging model. International Journal of Pressure Vessels and Piping, 170 (2019) 92-101.

[6]   G. Liu, Y. Li, Vibration analysis of liquid-filled pipelines with elastic constraints. Journal of Sound and Vibration, 330 (13) (2011) 3166-3181.

[7]   A. Kwong, K. Edge, A method to reduce noise in hydraulic systems by optimizing pipe clamp locations. Proceedings of the Institution of Mechanical Engineers. Part I, Journal of Systems and Control engineering, 212 (4) (1998) 267-280.

[8]   Y. Huang, Y. Liu, B. Li, Y. Li, Z. Yue, Natural frequency analysis of fluid conveying pipeline with different boundary conditions. Nuclear Engineering and Design, 240 (3) (2010) 461-467.

[9]   T.G. Ritto, C. Soize, F.A. Rochinha, R. Sampaio, Dynamic stability of a pipe conveying fluid with an uncertain computational model. Journal of Fluids and Structures, 49 (2014) 412-426.

[10]   H. Zhai, Z. Wu, Y. Liu, Z. Yue, The dynamic reliability analysis of pipe conveying fluid based on a refined response surface method. Journal of Vibration and Control, 21 (4) (2015) 790-800.

[11]   X. Guo, Y. Cao, H. Ma, C. Xiao, B. Wen, Dynamic analysis of an L-shaped liquid-filled pipe with interval uncertainty. International Journal of Mechanical Sciences, (2021) 107040.

[12]   J. Wu, A. Tijsseling, Y. Sun, Z. Yin, In-plane wave propagation analysis of fluid-filled L-Shape pipe with multiple supports by using impedance synthesis method. International Journal of Pressure Vessels and Piping, 188 (2020) 104234.

[13]   J. Herrmann, M. Maess, L. Gaul, Substructuring including interface reduction for the efficient vibro-acoustic simulation of fluid-filled piping systems. Mechanical Systems and Signal Processing, 24 (1) (2010) 153-163.

[14]   L. Wang, Y. Yang, Y. Li, Y. Wang, Resonance analyses of a pipeline-riser system conveying gas-liquid two-phase flow with flow-pattern evolution. International Journal of Pressure Vessels and Piping, 161 (2018) 22-32.

[15]   Q. Chai, J. Zeng, H. Ma, K. Li, Q. Hai, A dynamic modeling approach for nonlinear vibration analysis of the L-type pipeline system with clamps. Chinese Journal of Aeronautics, 33 (12) (2020) 3253-3265.

[16]   P. Gao, J. Li, J. Zhai, Y. Tao, Q. Han, A novel optimization layout method for clamps in a pipeline system. Applied Sciences, 10 (1) (2020) 390.

[17]   Z. Tang, Z. Lu, D. Li, F. Zhang, Optimal design of the positions of the hoops for a hydraulic pipelines system. Nuclear Engineering and Design, 241 (12) (2011) 4840-4855.

[18]   A. Keramat, M. Fathi-Moghadam, R. Zanganeh, M. Rahmanshahi, A.S. Tijsseling, E. Jabbari, Experimental investigation of transients-induced fluid–structure interaction in a pipeline with multiple-axial supports. Journal of Fluids and Structures, 93 (2020) 102848.

[19]   Y. Xu, D.N. Johnston, Z. Jiao, A.R. Plummer, Frequency modelling and solution of fluid–structure interaction in complex pipelines. Journal of Sound and Vibration, 333 (10) (2014) 2800-2822.

[20]   M.P. Païdoussis, T.P. Luu, B.E. Laithier, Dynamics of finite-length tubular beams conveying fluid. Journal of Sound and Vibration, 106 (2) (1986) 311-331.

[21]   Y.M. Ram, J.E. Mottershead, Multiple-input active vibration control by partial pole placement using the method of receptances. Mechanical Systems and Signal Processing, 40 (2) (2013) 727-735.

[22] B. Mokrani, F. Palazzo, J.E. Mottershead, S. Fichera, Multiple-input multiple-output experimental aeroelastic control using a receptance-based method. Aiaa Journal, 57 (7) (2019) 3066-3077.

[23] M. Ghandchi Tehrani, R.N.R. Elliott, J.E. Mottershead, Partial pole placement in structures by the method of receptances: Theory and experiments. Journal of Sound and Vibration, 329 (24) (2010) 5017-5035.

[24] J.E. Mottershead, Y.M. Ram, Inverse eigenvalue problems in vibration absorption: Passive modification and active control. Mechanical Systems and Signal Processing, 20 (1) (2006) 5-44.

[25] O. Çakar, Mass and stiffness modifications without changing any specified natural frequency of a structure. Journal of Vibration and Control, 17 (5) (2010) 769-776.

[26] H. Ouyang, D. Richiedei, A. Trevisani, Eigenstructure assignment in undamped vibrating systems：A convex-constrained modification method based on receptances. Mechanical Systems and Signal Processing, 27 (1) (2012) 397-409.

[27] H. Ouyang, D. Richiedei, A. Trevisani, G. Zanardo, Discrete mass and stiffness modifications for the inverse eigenstructure assignment in vibrating systems: Theory and experimental validation. International Journal of Mechanical Sciences, 64 (1) (2012) 211-220.

[28] H. Liu, H. Gao, Y. Ma, Receptance-based assignment of dynamic characteristics: A summary and an extension. Mechanical Systems and Signal Processing, 145 (2020) 106913.

[29] A. Kyprianou, J.E. Mottershead, H. Ouyang, Assignment of natural frequencies by an added mass and one or more springs. Mechanical Systems and Signal Processing, 18 (2) (2004) 263-289.

[30] D. Richiedei, I. Tamellin, A. Trevisani, Simultaneous assignment of resonances and antiresonances in vibrating systems through inverse dynamic structural modification. Journal of Sound and Vibration, 485 (2020) 115552.

[31] S. Zhang, H. Ouyang, Receptance-based frequency assignment for assembled structures. Journal of Vibration and Control, (2020) 1802394799.

[32] J.E. Mottershead, M. Ghandchi Tehrani, D. Stancioiu, S. James, H. Shahverdi, Structural modification of a helicopter tailcone. Journal of Sound and Vibration, 298 (1-2) (2006) 366-384.

[33] O. Zarraga, I. Ulacia, J.M. Abete, H. Ouyang, Receptance based structural modification in a simple brake-clutch model for squeal noise suppression. Mechanical Systems and Signal Processing, 90 (2017) 222-233.

[34] S. Tsai, H. Ouyang, J. Chang, Inverse structural modifications of a geared rotor-bearing system for frequency assignment using measured receptances. Mechanical Systems and Signal Processing, 110 (2018) 59-72.

[35] S. Li, B.W. Karney, G. Liu, FSI research in pipeline systems - a review of the literature. Journal of Fluids and Structures, 57 (2015) 277-297.

[36] S. Shah, M.P. Mignolet, Effects of structural-fluid coupling uncertainty on the dynamic behavior of nominally straight and uniform pipes conveying fluid: Modeling and numerical study. Journal of Fluids and Structures, 85 (2019) 55-76.

[37] L. Wang, X. Wang, Y. Li, J. Hu, A non-probabilistic time-variant reliable control method for structural vibration suppression problems with interval uncertainties. Mechanical Systems and Signal Processing, 115 (2019) 301-322.

[38] L. Wang, J. Liu, C. Yang, D. Wu, A novel interval dynamic reliability computation approach for the risk evaluation of vibration active control systems based on PID controllers. Applied Mathematical Modelling, 92 (2021) 422-446.

[39] C. Jiang, X. Han, F.J. Guan, Y.H. Li, An uncertain structural optimization method based on nonlinear interval number programming and interval analysis method. Engineering Structures, 29 (11) (2007) 3168-3177.

[40] K. Deb, A. Pratap, S. Agarwal, T. Meyarivan, A fast and elitist multiobjective genetic algorithm: NSGA-II. Ieee Transactions On Evolutionary Computation, 6 (2) (2002) 182-197.

[41] H.L. Dai, L. Wang, Q. Qian, J. Gan, Vibration analysis of three-dimensional pipes conveying fluid with consideration of steady combined force by transfer matrix method. Applied Mathematics and Computation, 219 (5) (2012) 2453-2464.

[42] H. Farokhi, M. Tavallaeinejad, M.P. Païdoussis, Geometrically exact dynamics of cantilevered pipes conveying fluid. Journal of Fluids and Structures, 106 (2021) 103364.

[43] G. Koo, Y. Park, Vibration analysis of a 3-dimensional piping system conveying fluid by wave approach. International Journal of Pressure Vessels and Piping, 67 (1996) 249-256.

[44] Y. Cao, Q. Chai, X. Guo, H. Ma, P. Wang, Comparative study on two finite element models for multi-clamp pipeline system. Journal of Mechanical Science and Technology, (2022).

[45] G. Liu, S. Li, Y. Li, H. Chen, Vibration analysis of pipelines with arbitrary branches by absorbing transfer matrix method. Journal of Sound and Vibration, 332 (24) (2013) 6519-6536.

[46] H.K. Aliabadi, A. Ahmadi, A. Keramat, Frequency response of water hammer with fluid-structure interaction in a viscoelastic pipe. Mechanical Systems and Signal Processing, 144 (2020) 106848.

[47] H. Ouyang, L. Baeza, S. Hu, A receptance-based method for predicting latent roots and critical points in friction-induced vibration problems of asymmetric systems. Journal of Sound and Vibration, 321 (3-5) (2009) 1058-1068.

[48] D. Ewins, Modal testing, theory, practice and application, second ed. Mechanical Engineering Research Studies: Engineering Dynamics Series, Research Studies Press, Baldock, England, 2000.

[49] K. Deb, Multi-objective optimization using evolutionary algorithms, John Wiley and Sons, Ltd, Chichester, England, 2001.

[50] L. Wang, X. Wang, Y. Li, G. Lin, Z. Qiu, Structural time-dependent reliability assessment of the vibration active control system with unknown-but-bounded uncertainties. Structural Control and Health Monitoring, 24 (10) (2017) e1965.

[51] L. Zhang, T. Zhang, H. Ouyang, T. Li, Receptance-based antiresonant frequency assignment of an uncertain dynamic system using interval multiobjective optimization method. Journal of Sound and Vibration, (2022) 116944.

[52] F. Li, G. Sun, X. Huang, J. Rong, Q. Li, Multiobjective robust optimization for crashworthiness design of foam filled thin-walled structures with random and interval uncertainties. Engineering Structures, 88 (2015) 111-124.

[53] T. Zhang, H. Ouyang, Y.O. Zhang, B.L. Lv, Nonlinear dynamics of straight fluid-conveying pipes with general boundary conditions and additional springs and masses. Applied Mathematical Modelling, 40 (17-18) (2016) 7880-7900.

[54] D.J. Ewins, A method for modal identification of light damped structures. Journal of Sound and Vibration, 1 (84) (1982) 57-79.

[55] J. Herrmann, T. Haag, L. Gaul, Experimental and numerical investigation of the dynamics in spatial fluid-filled piping systems. The Journal of the Acoustical Society of America, 123 (5) (2008) 3422.

[56] R. Caracciolo, D. Richiedei, I. Tamellin, Robust assignment of natural frequencies and antiresonances in vibrating systems through dynamic structural modification. Shock and Vibration, 2021 (2021) 1-20.

[57] Cylindrical coiled compression spring dimensions and parameters (in Chinese), GB/T 2089-2009.